

# Soft Matter

Accepted Manuscript



This is an *Accepted Manuscript*, which has been through the Royal Society of Chemistry peer review process and has been accepted for publication.

*Accepted Manuscripts* are published online shortly after acceptance, before technical editing, formatting and proof reading. Using this free service, authors can make their results available to the community, in citable form, before we publish the edited article. We will replace this *Accepted Manuscript* with the edited and formatted *Advance Article* as soon as it is available.

You can find more information about *Accepted Manuscripts* in the [Information for Authors](#).

Please note that technical editing may introduce minor changes to the text and/or graphics, which may alter content. The journal's standard [Terms & Conditions](#) and the [Ethical guidelines](#) still apply. In no event shall the Royal Society of Chemistry be held responsible for any errors or omissions in this *Accepted Manuscript* or any consequences arising from the use of any information it contains.

# Humidity-Dependent Compression-Induced Glass Transition of the Air-Water Interfacial Langmuir Films of Poly(D,L-lactic acid-*ran*-glycolic acid) (PLGA)

Hyun Chang Kim,<sup>a</sup> Hoyoung Lee,<sup>a</sup> Hyunjung Jung,<sup>b</sup> Yun Hwa Choi,<sup>a</sup> Mati Meron,<sup>c</sup>  
Binhua Lin,<sup>c</sup> Joona Bang,<sup>b</sup> You-Yeon Won<sup>a,\*</sup>

<sup>a</sup> School of Chemical Engineering, Purdue University, West Lafayette, Indiana 47907

<sup>b</sup> Department of Chemical and Biological Engineering, Korea University, Seoul, Korea 136-713

<sup>c</sup> Advanced Photon Source, University of Chicago, Chicago, Illinois 60439

Keywords: poly(D,L-lactic acid-*ran*-glycolic acid) (PLGA), glass transition, Langmuir film, Langmuir monolayer, humidity

## ABSTRACT

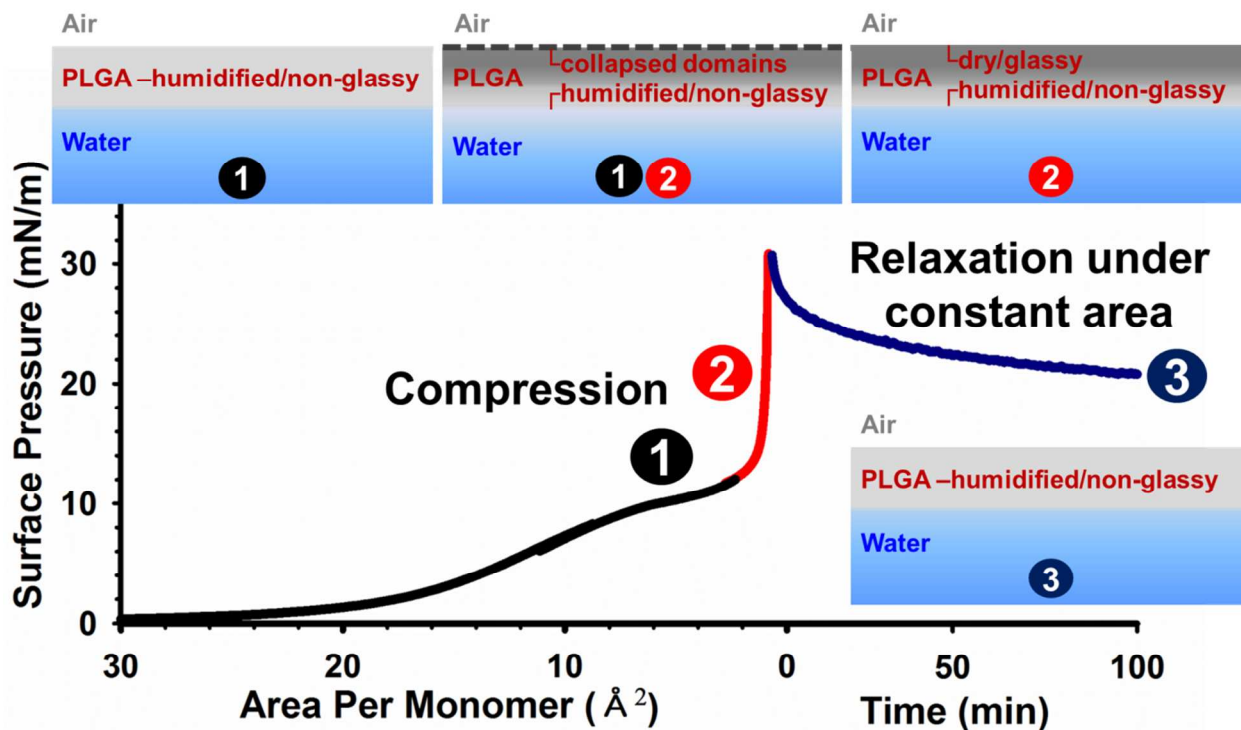
Constant rate compression isotherms of the air-water interfacial Langmuir films of poly(D,L-lactic acid-*ran*-glycolic acid) (PLGA) show a distinct feature of having an exponential increase

---

\* To whom correspondence should be addressed. E-mail: yywon@ecn.purdue.edu

in surface pressure in the high surface polymer concentration regime. We have previously demonstrated that this abrupt upturn in surface pressure is linked to the glass transition of the polymer film, but the detailed mechanism of this process had not been fully understood. In order to obtain molecular-level understanding of this behavior, we performed extensive characterizations of the surface mechanical, structural and rheological properties of Langmuir PLGA films at the air-water interface, using combined experimental techniques including the Langmuir film balance, X-ray reflectivity and double-wall-ring interfacial rheometry methods. We observed that the mechanical and structural responses of the Langmuir PLGA film are significantly dependent upon the rate of film compression; the glass transition was induced in the PLGA film only at fast compression rates. Surprisingly, we found that this deformation rate dependence is also dependent upon the humidity of the environment. With water acting as a plasticizer for the PLGA material, the diffusion of water molecules through the PLGA film appears to be the key factor determining the glass transformation property and thus the mechanical response of the PLGA film against lateral compression. Based on our combined results, we hypothesize the following mechanism for the compression-induced glass transformation of the Langmuir PLGA film; (1) initially, a humidified/non-glassy PLGA film is formed in the full surface-coverage region (where the surface pressure shows a plateau) during compression; (2) further compression leads to the collapse of the PLGA chains and the formation of new surfaces on the air side of the film, and this newly formed top layer of the PLGA film is transiently glassy in character because the water evaporation rate in the top surface region is momentarily faster than the humidification rate (due to the initial roughness of the newly formed surface); (3) after some period of time, the top layer itself becomes humidified through diffusion

of water from the subphase, and thus it becomes non-glassy, leading to the relaxation of the applied compressive stress.



## 1. Introduction

Confinement of polymers into small thicknesses can dramatically alter their physical properties (e.g., thermo-mechanical and rheological properties).<sup>1, 2</sup> One method of producing molecularly thin layers of polymers is to spread a polymer on a water surface; this process results in the formation of a so-called Langmuir polymer monolayer. For formation of a stable (i.e., insoluble but well-spread) monolayer, it is necessary for the polymer to possess an amphiphilic repeat unit structure. The hydrophobic groups within the repeat unit structure make the polymer insoluble in water and thus help the polymer settle at the air-water interface. The hydrophilic groups enhance the spreading of the polymer on the water surface. When compressed, a “stable” monolayer

(formed by polymers possessing “amphiphilic” character) transforms into a multi molecular layer.<sup>3</sup>

Using the Langmuir film balance technique, the surface/interfacial tension of a Langmuir polymer monolayer can be measured as a function of monolayer area. The surface/interfacial tension ( $\gamma$ ) is defined as the amount of free energy required to increase the surface/interface area by a unit amount at constant temperature and pressure, that is,  $\gamma = \left(\frac{\partial G}{\partial A}\right)_{T,P}$ . From this monolayer interfacial tension, the surface pressure of the monolayer ( $\pi$ ) can be calculated by  $\pi = \gamma_{\text{air-water}} - \gamma_{\text{air-polymer-water}}$ . A surface pressure ( $\pi$ ) versus mass concentration ( $\Gamma$ ) isotherm of a Langmuir polymer monolayer typically consists of two regimes: the chain expanded regime at low surface polymer concentrations, and the chain collapse regime at high surface polymer concentrations. The chain expanded regime can be divided into three sub-regimes, i.e., dilute, semi-dilute, and concentrated (analogously to de Gennes’ categorization of concentration regimes of polymer solutions).<sup>4</sup>

The “chain expanded” regime has been well studied in polymer monolayers. In the “dilute” concentration regime, individual chains exist as isolated objects in two-dimensional (2D) space. A non-ideal dependence of surface pressure on surface concentration can be described by the virial equation of state  $\pi = \frac{RT\Gamma}{M_n} (1 + A_2\Gamma + \dots)$  where  $A_2$  denotes the second virial coefficient which is a measure of the two-body interaction between the monomer groups, and  $M_n$  is the number-average molecular weight of the polymer.<sup>5</sup> In the “semi-dilute” regime, the polymer chains overlap one another, and the surface pressure no longer depends on the molecular weight of the polymer but it only depends on the surface monomer concentration (i.e., the polymer mass concentration).<sup>6</sup> A de Gennes-type scaling theory suggests a power law relationship between the surface pressure and the polymer mass concentration  $\pi \propto \Gamma^y$  where the scaling exponent ( $y$ ) is

related to the 2D Flory exponent ( $\nu$ ) by  $y = \frac{2\nu}{2\nu-1}$ . The 2D Flory exponent is a parameter that characterizes the effective “solvent quality” of the surrounding medium that the polymer chains experience at the air-water interface.<sup>7</sup> Mean-field theory predicts a Flory exponent of 0.75 for a good solvent system.<sup>8</sup> A numerical analysis suggests a value of  $\nu = 0.505$  at the theta condition.<sup>9</sup> These predictions are well supported by experiment.<sup>10-13</sup> Our laboratory has also performed experimental investigations in this area and found, for instance, a 2D Flory exponent of  $\nu \approx 0.57$  for poly(*n*-butyl acrylate) (PnBA)<sup>4</sup> and a 2D Flory exponent of  $\nu \approx 0.76$  for poly(D,L-lactic acid-*ran*-glycolic acid) (PLGA).<sup>14</sup>

The “chain collapsed” regime is where the polymer chains are no longer in the monomolecular layer state. Excess material forms collapsed multi-layered regions; thus in this state the system is more appropriately referred to as a “Langmuir polymer film”. Thus, during monolayer compression, this chain collapsed regime starts at the surface polymer concentration corresponding to the full surface coverage condition.<sup>4</sup> In 1946, Crisp reported extensive data comparing surface pressure-area isotherm data for a wide range of different polymers; amorphous fluid-like polymers typically exhibit flat surface pressure profiles at low area per chain conditions, whereas amorphous tough/brittle polymers and semi-crystalline polymers typically exhibit rapid increases in surface pressure under compression at low areas.<sup>15, 16</sup> However, the exact molecular mechanisms responsible for these solid-like mechanical responses exhibited by highly compressed films of glassy/crystalline polymers remain to be better elucidated.

Our laboratory has performed extensive experimental studies on the air-water monolayers/films of (non-glassy) PnBA, which has been categorized by Crisp as an “amorphous fluid-like” (Group I) polymer, and (glassy) PLGA, which can be categorized as an “amorphous

brittle” (Group II) polymer according to the classification of Crisp.<sup>4, 14</sup> From the results of these studies we concluded that Langmuir PLGA (Group II) films typically exhibit rapid increases in surface pressure under high compression because of a transformation of the material into a glassy state. This explanation was also supported by the observation that a Langmuir film formed by poly(D,L-lactic acid-*ran*-glycolic acid-*ran*-caprolactone) (PLGACL), which is similar in chemical structure to PLGA but is non-glassy due to the presence of the caprolactone co-monomer units, exhibits a surface pressure behavior similar to PnBA at low area conditions.<sup>14</sup> Furthermore, liquid atomic force microscopy (AFM) images suggested that collapsed domains within highly compressed PLGA films assume laterally inter-connected morphologies (although it is a question how closely the Langmuir-Blodgett-deposited AFM samples represent the natural (air-water interfacial) state of the Langmuir films).<sup>14</sup> In the present study, we intend to deepen our understanding regarding the molecular mechanisms responsible for the processes of film collapse and glass transformation occurring in highly compressed Langmuir PLGA films. For this purpose, we examine the dependence of the surface pressure-area compression isotherms of PLGA monolayers/films on various parameters such as temperature, compression speed, preparation condition, and relaxation time. We also investigate the molecular structural characteristics of Langmuir PLGA films under various states of compression by X-ray reflectivity (XR). The results of these experiments suggest that the humidity of the surrounding environment is an important factor that influences the surface mechanical properties of Langmuir PLGA films. Isotherm measurements under varying humidity environments further support this view. In the context of understanding the effect of preparation condition on the structural state of the PLGA film, we also characterized the interfacial rheological properties of Langmuir PLGA films.

## 2. Experimental Procedures

### 2.1 Materials

An ester-terminated PLGA homopolymer with an inherent viscosity of 0.40 ( $\pm$  0.14) dl/g and a lactic acid-glycolic acid ratio of 50:50 was purchased from Lactel; its number-average molecular weight has been measured by  $^1\text{H}$  NMR to be 17.1 kg/mol. This 17.1-kDa PLGA was used in all measurements reported in this paper except for the data shown in Figure 7(c) for which a higher molecular weight PLGA (number-average molecular weight = 49.1 kg/mol, inherent viscosity = 0.85 ( $\pm$  0.09) dl/g, lactic acid:glycolic acid = 50:50, purchased from Lactel) was used. HPLC grade chloroform (99.8%, containing 0.5 – 1.0 % ethanol as stabilizer, Sigma Aldrich) was used as the initial spreading solvent for the preparation of PLGA Langmuir films. Deionized Millipore-purified water (18 M $\Omega$ ·cm resistivity) was used as the subphase.

### 2.2 Surface Pressure-Area Isotherms

Constant compression rate surface pressure-area isotherms of Langmuir PLGA films were measured using a KSV 5000 double barrier Langmuir trough with dimensions of 15 cm (width) by 51 cm (length) placed in a Plexi glass environmental isolation chamber. The temperature of the subphase was controlled by a circulating water bath (the circulating water flows through a jacket located beneath the trough), and was measured using a thermocouple placed in contact with the subphase. The surface pressure was measured using a platinum Wilhelmy plate probe located at the center of the trough. In all measurements we initially aligned the Wilhelmy plate perpendicular to the barriers. However, when a Langmuir film is compressed at a high speed or when the measurement involves a glassy film (such as the one formed by PLGA), the Wilhelmy

plate typically rotates during the measurement. (Also of note, in X-ray reflectivity (XR) measurements performed at Argonne National Laboratory, the orientation of the Wilhelmy plate was typically prone to change due to the movement of the entire sample stage.) Nevertheless, the drift in Wilhelmy probe orientation during measurement (typically less than 20 degrees in angle) was confirmed to produce insignificant influences on the data; as shown in Figure S1 of Electronic Supplementary Information (ESI), the two different orientations of the Wilhelmy plate (i.e., perpendicular vs. parallel relative to the barrier orientation) only produce a negligible difference in the isotherm data (< about 6 mN/m at maximum). This small uncertainty associated with the Wilhelmy probe orientation does not influence any of the main points or conclusions in this article. The probe was cleaned by washing with ethanol and water (three times with each solvent) and then by flaming using a propane torch for about 10 seconds for each side. Before measurement the surfaces of the trough and barriers were cleaned by washing with ethanol and water (three times with each solvent). Before spreading the polymer, the surface of the subphase water was vacuum aspirated to remove trace amounts of contaminants. Literature values of water surface tensions at several different measurement temperatures were used to confirm the preciseness of the surface pressure measurements for the given temperature conditions;<sup>17</sup> calibrations for surface pressure measurements were performed to within  $\pm 0.5$  mN/m (measurement errors are due to thermal fluctuations and variations of the probe condition). Chloroform was used as the spreading solvent. The PLGA spreading solution was prepared a day before use. A calculated amount (typically 60  $\mu$ l) of the spreading solution (a 5, 10, 15 or 20 mg/ml PLGA solution in chloroform) was added drop-wise to the surface of the water subphase; a drop was formed at the tip of a Hamilton microsyringe needle, and was made in gentle contact with the surface of the water. The surface pressure decrease was monitored over time after the

spreading of the polymer (i.e., during the evaporation of chloroform) and compared with the change in the surface pressure of an empty water surface measured over time in order to determine the appropriate start point for the surface pressure-area isotherm measurement; the surface pressure of blank water itself very slowly decreases with time (at a slope of about - 0.05375 mN/m/h in a typical humidity-uncontrolled environment) due to slow evaporation of water, which lowers the meniscus of the water in contact with the Wilhelmy probe. It generally takes about 90 minutes for the spreading solvent (chloroform) to evaporate completely. Typical surface pressure-area isotherm measurement conditions used were: a compression rate of 3 mm/min, and 50 – 60% relative humidity (unless stated otherwise). All isotherm data presented in this paper were reproducible for independent repeated trials (at least three times) to within about 5 % variation in the surface pressure or area per monomer (or area per chain) values.

### 2.3 X-Ray Reflectivity

X-ray reflectivity (XR) measurements were conducted at the ChemMatCARS beamline 15-ID-C at U.S. Department of Energy Office of Science's Advanced Photon Source (APS) (Argonne, Illinois). The XR instrument was equipped with a custom designed one barrier Langmuir trough with dimensions of 98 mm (width) by 350 mm (length). A filter paper probe of 1 cm width was used for surface pressure measurements. The surrounding environment was maintained in a dry helium atmosphere (to minimize background X-ray scattering from air). The Langmuir trough equipment was placed on a vibration isolation table. An incident X-ray radiation at a wavelength of 1.25 Å was used, and XR profiles were measured in the out-of-plane momentum transfer vector ( $q_z$ ) range of 0.016 – 0.700 Å<sup>-1</sup>. The spatial resolution was about 4.5 Å. The X-ray

exposure of the sample was limited to  $1.5 \times 10^{13}$  photons/mm<sup>2</sup> to avoid any artifact associated with X-ray-induced beam damage. All other details were the same as in Ref. 18.

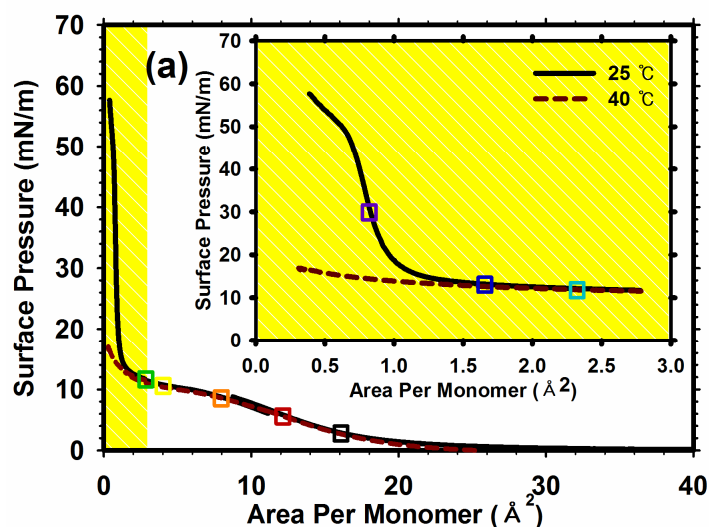
## 2.4 Interfacial Rheology

Interfacial rheological properties of Langmuir PLGA films were measured using a double wall ring (DWR) fixture on a stress-controlled DHR-2 rheometer (TA Instruments). The DWR trough was placed on a Peltier plate to control the temperature. An external thermocouple was used to monitor the subphase temperature. To avoid water evaporation during the measurement a sealed environment was constructed surrounding the DWR system. Prior to each set of measurements on a monolayer sample, the “Oscillatory Mapping” of the “DWR Geometry” was performed using the “Precision Mapping” option in two iterations. The DWR trough was loaded with 20 ml of Millipore water, and the surface of this subphase water was cleaned by vacuum aspiration. The PLGA spreading solution in chloroform was applied drop-wise to the surface of the subphase, and the chloroform solvent was allowed to evaporate for about 90 minutes. When the sample was ready for measurement, the upper DWR fixture was lowered until it made initial contact with the water; this point was determined by visual observation of the water surface. Afterwards, the fixture was further lowered by 500  $\mu\text{m}$  in order to locate the edges of the DWR exactly at the air-water interface. For steady shear rate sweep measurements, the viscosity data were accepted as steady state for a given shear rate only when the viscosity values from three consecutive runs agreed within 5 % variation. The viscosity sampling period was 500 seconds, and the maximum equilibration time was 10,000 seconds per shear rate step. For linear oscillatory frequency sweep measurements, the effect of inertia was often non-negligible, and measurements were considered valid only at oscillatory frequencies at which raw phase angles

were below 175 degrees. The applied torque was set at  $0.5 \mu\text{N}\cdot\text{m}$ , which was (in a separate test) confirmed to be within the linear viscoelastic range for the Langmuir PLGA film at the  $0.8 \text{ \AA}^2$  per monomer condition. In all frequency sweep measurements, the torque values were confirmed to vary within 2 % deviation from the set point. A freshly prepared PLGA monolayer sample was used for each run. Also, if a measurement took longer than 24 hours to complete, a replicate sample was prepared afresh for continuation of the measurement, because of the slow evaporation of the water. The position of the air-water interface was checked after each measurement to insure that the amount of water evaporation during the measurement was negligible.

### 3. Results and Discussion

#### 3.1 Temperature Dependence of the PLGA Compression Isotherm



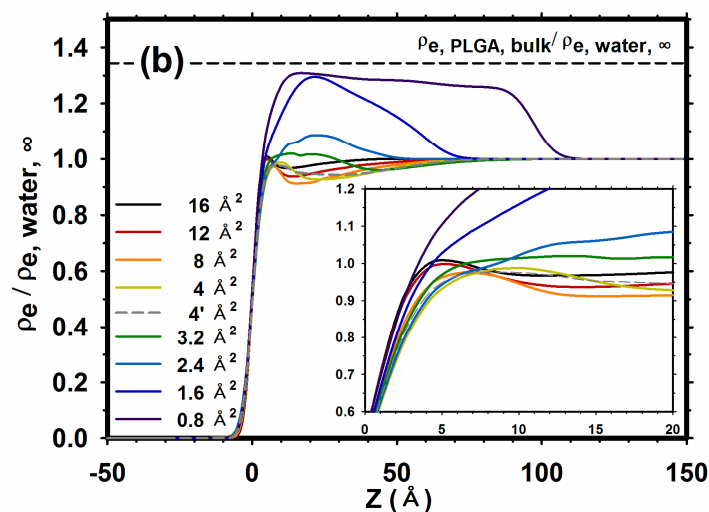


**Figure 1.** (a) Constant compression rate isotherm curves of a PLGA monolayer at 25 and 40 °C (PLGA molecular weight: 17.1 kDa). The inset shows a magnification of the yellow highlighted region. (b) The electron density profiles of the Langmuir PLGA film measured by X-ray reflectivity (XR) at the different area per monomer conditions marked with open squares in (a); the original XR data are shown in Figure S2. Due to a trough compression ratio limitation, the XR measurements were performed in two runs; i.e., one set of measurements were performed during compression of the monolayer prepared at 16 Å<sup>2</sup> per monomer to an area of 4 Å<sup>2</sup> per monomer, and a second set of measurements during compression from an initial area of 4 Å<sup>2</sup> per monomer to 0.8 Å<sup>2</sup> per monomer (the data corresponding to the 4 Å<sup>2</sup> starting condition are denoted with “4’ Å<sup>2</sup>” in the legend). The PLGA film thicknesses determined from the data shown in (a) agree well with the values calculated based on the bulk density of PLGA (1.58 g/cc) (Figure S3), supporting the reasonableness of the electron density profiles shown in (b).

Constant compression rate isotherms of PLGA were measured at two different temperatures of 25 and 40 °C. As shown in Figure 1(a), a typical PLGA constant compression rate isotherm shows a slow increase in surface pressure at high area per monomer (8 – 30 Å<sup>2</sup>) leading to a plateau region at intermediate area per monomer (2 – 8 Å<sup>2</sup>) and an exponential up rise at low area per monomer (< 2 Å<sup>2</sup>). Overall, the isotherm curves at the two temperatures were identical except in the low area per monomer region where there was a significant deviation. The inset of Figure 1(a) clearly shows that the PLGA isotherm measured at 25 °C shows a sharp up rise in surface pressure in the low area per monomer region, while no such behavior is observed at 40 °C. This

exponential increase in surface pressure has been speculated to be caused by the glass transition behavior of PLGA.<sup>14</sup> Bulk (dry) PLGA has a glass transition temperature of about 45 °C.<sup>14,19</sup> At 40 °C, which is below the glass transition temperature of bulk PLGA, the PLGA in the form of a Langmuir air-water interfacial film appears to assume a non-glassy character. Another interesting observation was that at 25 °C when the compression was stopped at an area per monomer below 2 Å<sup>2</sup>, the surface pressure started to drop rapidly, whereas at 40 °C the surface pressure remained constant even after the compression was stopped (Figure S4). This result suggests that the change in the molecular state of the PLGA that occurs under high compression at 25 °C, for some reason, is only transient in nature, and the change is reversed when its driving force is removed. The work reported in this paper was in fact undertaken in an attempt to propose an explanation for this observation.

The out-of-plane electron density profiles of the Langmuir PLGA film were measured by X-ray reflectivity (XR) at several different area per monomer conditions; the results are displayed in Figure 1(b). At each area per monomer condition, XR measurements were repeated twice on two different X-ray exposure locations of the polymer film to confirm reproducibility. Notably, as shown in the figure, at a monolayer area of 4 Å<sup>2</sup> per monomer, the compressed versus as-spread Langmuir film samples (i.e., the Langmuir PLGA film compressed from 16 to 4 Å<sup>2</sup> per monomer vs. the PLGA film as it has been prepared at the 4 Å<sup>2</sup> per monomer condition) exhibited electron density profiles that are only slightly dissimilar but mostly alike. At this area condition (4 Å<sup>2</sup> per monomer) the monolayer morphology appears to be largely unaffected by the preparation history; at this area condition the surface pressure of the monolayer was also largely unaffected by the monolayer preparation method (i.e., isotherm curves obtained over different ranges of area overlapped nicely with one another in this intermediate area per monomer region;

data not shown). The monolayer electron density profiles at 16 and 12  $\text{\AA}^2$  per monomer show that at these conditions the PLGA layer has thicknesses on the order of several  $\text{\AA}$  which is comparable to the physical size of the PLGA monomer unit ( $\approx 5 \text{\AA}^{20}$ ), suggesting that the PLGA chains do exist as (close to) two-dimensional objects. The thickness of the PLGA monolayer continues to increase as the monolayer area is reduced. The maximum electron density of the PLGA film at 1.6 and 0.8  $\text{\AA}^2$  per monomer becomes noticeably higher than at higher areas. The maximum electron density reaches the 97.7 percent level of the bulk glassy PLGA density (as can be seen from Figure 1(b)), which supports the film glass transition scenario. This result is also consistent with the observation that at these area per monomer conditions (particularly, at 0.8  $\text{\AA}^2$  per monomer), the Langmuir PLGA film shows a solid-like mechanical resistance to compression (i.e., a sharp up rise in surface pressure in response to compression). Also, very interestingly, in these situations, the PLGA electron density profiles typically show higher density values on the air side of the Langmuir PLGA film than the rest of the regions, which suggests that the glassy domains are formed preferentially near the air surface; this point will also be discussed in Section 3.4 with reference to the data presented in Figure 5.

We would like to point out that there is no theoretical or logical basis upon which to predict that the  $T_g$  of the air-water interfacial films of PLGA should be significantly lower than that of bulk PLGA simply because of reduced thickness (in analogy to free-standing film situations). The available data in the literature suggest that, in fact, the  $T_g$  of a polymer film can increase, decrease, or even remain unchanged with decreasing thickness, depending on the nature of the interaction between the polymer and the substrate (as discussed, for instance, in Ref. 21). The energetic interactions between water molecules and PLGA will, therefore, control the interfacial

behavior of the polymer. To our knowledge, the  $T_g$  of a Langmuir polymer film has never been directly measured.

### 3.2 Dynamic Nature of the Surface Pressure Increase at High Compression

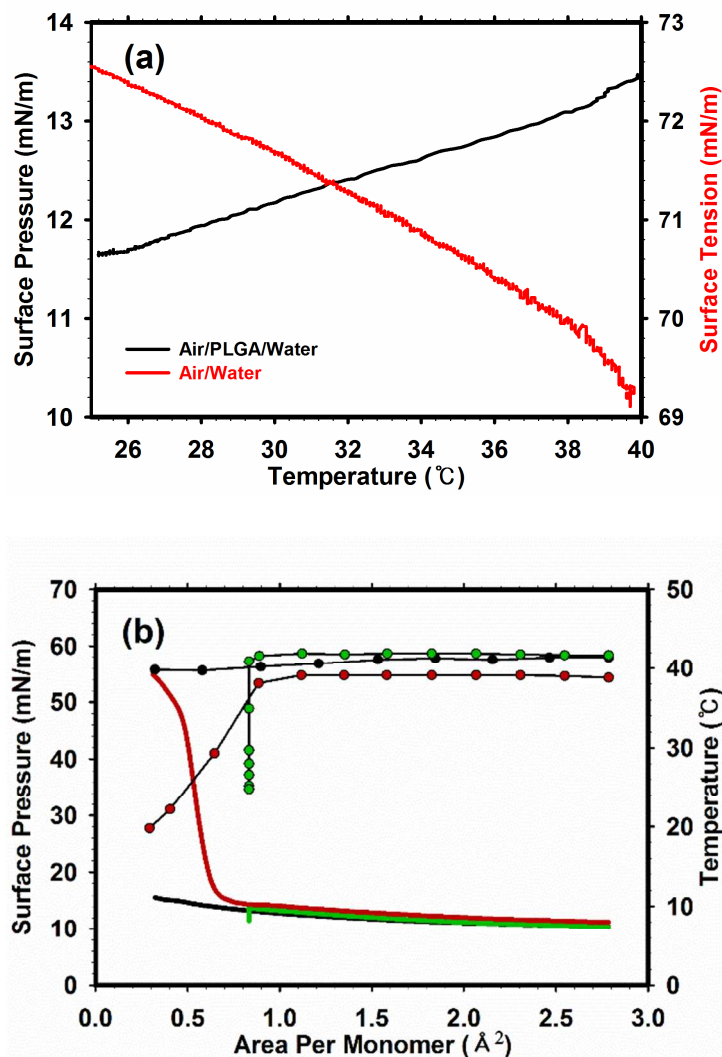


**Figure 2.** (a) Surface pressure of a Langmuir PLGA film system (initially prepared by spreading the polymer onto the water surface to a surface polymer concentration corresponding to  $0.8 \text{ \AA}^2$  per monomer at  $40 \text{ }^\circ\text{C}$ ) measured at a constant monolayer area of  $0.8 \text{ \AA}^2$  per monomer during cooling from  $40$  to  $25 \text{ }^\circ\text{C}$  (black curve). Water surface tension measured during cooling from  $40$  to  $25 \text{ }^\circ\text{C}$  (red curve). (b) Surface pressures of a Langmuir PLGA film under continuous compression at  $40 \text{ }^\circ\text{C}$  (black curve), of a Langmuir PLGA film that was initially compressed to an area of  $0.8 \text{ \AA}^2$  per monomer at a constant temperature of  $40 \text{ }^\circ\text{C}$  and then cooled down to  $25 \text{ }^\circ\text{C}$

at a constant area of  $0.8 \text{ \AA}^2$  per monomer (green curve), and of a Langmuir PLGA film that was initially compressed to an area of  $0.8 \text{ \AA}^2$  per monomer at a constant temperature of  $40 \text{ }^\circ\text{C}$  and then further compressed to a smaller area while the temperature was being reduced to  $25 \text{ }^\circ\text{C}$  starting at the  $0.8 \text{ \AA}^2$  per monomer point (red curve). In all cases, Langmuir film compression was performed at a rate of  $3 \text{ mm/min}$ .

In a previous publication,<sup>14</sup> we speculated that the exponential rise in surface pressure observed at low film areas originates from the interconnected glassy PLGA domains that form within the polymer film under high compression. However, this understanding is incomplete; as will be demonstrated by the data presented in this subsection, the change in the PLGA structure – whatever it is – that causes the surface pressure upturn is produced only during compression (and as shown in Figure S4 that change is only short lived afterwards if the compression is stopped). We start this discussion by noting that at  $40 \text{ }^\circ\text{C}$  (unlike at  $25 \text{ }^\circ\text{C}$ ) at all area conditions examined the monolayer pressure is unaffected by the monolayer compression history; the compressed versus as-spread samples produce identical values of surface pressure for a given area per monomer value (data not shown), suggesting that the compression history-dependent surface pressure behavior is a manifestation of the glassy film state at lower temperatures. However, it appears that low temperature itself is not the only condition for a Langmuir PLGA film to undergo glass transformation. For instance, if a Langmuir PLGA film is prepared at  $40 \text{ }^\circ\text{C}$  at an area of  $0.8 \text{ \AA}^2$  per monomer and then the temperature of the system is lowered from  $40 \text{ }^\circ\text{C}$  to  $25 \text{ }^\circ\text{C}$ , this process does not produce an up rise in surface pressure; in fact, the opposite happens (i.e., the surface pressure slightly decreases), as shown in Figure 2(a). The final surface pressure of this cooled down sample ( $\approx 11.6 \text{ mN/m}$  at  $0.8 \text{ \AA}^2$  per monomer) is identical to the surface pressure value obtained with an as-spread sample prepared directly at this temperature condition ( $25 \text{ }^\circ\text{C}$ ). Also shown in Figure 2(a) for comparison is the deionized water surface tension data obtained over the same temperature range. Obviously, the PLGA surface pressure changes in the

opposite direction to the change in the water surface tension as the system is cooled from 40 to 25 °C. Note that in the full surface coverage regime the plateau surface pressure is equivalent to the difference in the interfacial tension quantities,  $\pi_o = \gamma_{\text{air-water}} - (\gamma_{\text{air-polymer}} + \gamma_{\text{polymer-water}})$ .<sup>22, 23</sup> Using this concept and the data in Figure 2(a), we estimated a value of +5.2 mN/m for the change in the combined  $\gamma_{\text{air-polymer}}$  and  $\gamma_{\text{polymer-water}}$  interfacial tension due to the change in temperature from 40 to 25 °C; that is,  $\Delta(\gamma_{\text{air-polymer}} + \gamma_{\text{polymer-water}}) = \Delta\gamma_{\text{air-water}} - \Delta\pi_o = 3.4 + 1.8$  (mN/m).

To further confirm the necessary role of compression in inducing the glass transition in Langmuir PLGA films, we also performed the following additional tests. In one experiment, the PLGA monolayer was first compressed from an initial area of 2.8 Å<sup>2</sup> per monomer to a final area of 0.8 Å<sup>2</sup> per monomer at 40 °C, and then cooled down to 25 °C at a rate of about 0.9 °C/min while the area was kept constant at 0.8 Å<sup>2</sup> per monomer. As shown in Figure 2(b) (green curve), we did not observe any rise in surface pressure; similarly to Figure 2(a), the monolayer pressure in fact decreased by 1.85 mN/m. It should be noted that it is possible that a significant amount of stress should have already relaxed during this cooling period ( $\approx 1,000$  s); any surface pressure increase associated with the glass transition of the PLGA film during the cooling process might have been cancelled out by the effect of time-dependent stress relaxation. However, as demonstrated in Figure S4, even after the relaxation process is completed at 25 °C, there typically remains a residual stress, and the final surface pressure is always greater than the surface pressure value measured at 40 °C; therefore, if low temperature alone could cause the glass transformation of a Langmuir PLGA film, the cooling process should still produce an increase in surface pressure. In fact, the opposite is observed (i.e., the surface pressure decreases

as the temperature was lowered from 40 to 25 °C). In a different experiment, the monolayer was first compressed from 2.8 to 0.8 Å<sup>2</sup> per monomer at 40 °C, and when the area reached the 0.8 Å<sup>2</sup> value, the temperature setting was changed to 25 °C (the system started cooling at that point) while the film continued to be compressed at the same rate (3 mm/min). The surface pressure trace for this situation is shown as the red curve in Figure 2(b); as shown in the figure, this procedure produced a sharp rise in surface pressure. These results clearly indicate that mechanical deformation (i.e., lateral compression) is a required process in order for the Langmuir PLGA film to produce a solid-like material response (i.e., a sharp up slope in the isotherm curve), and this effect is operative only when the temperature is sufficiently low ( $\lesssim$  35 °C).

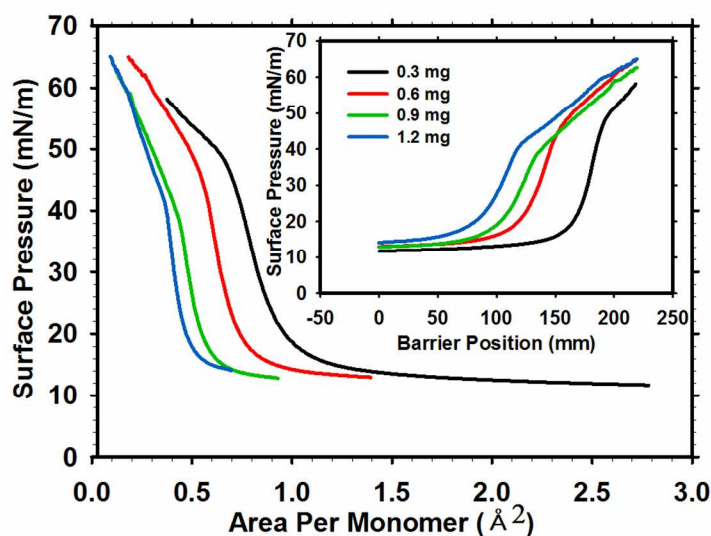


**Figure 3.** Surface pressure-area compression isotherms of Langmuir PLGA films prepared at different initial PLGA surface concentrations (PLGA molecular weight: 17.1 kDa). The PLGA films were compressed at a constant rate of 3 mm/min. The numbers shown in the legend denote the amounts of PLGA spread over the trough area of 75,750 mm<sup>2</sup>. Shown in the inset are the isotherm data replotted in the form of surface pressure vs. barrier position.

These observations suggest that the exponential increase in Langmuir film pressure at high compression is of dynamic/mechanical nature. Therefore, it is anticipated that the onset point (in area per monomer) for the rapid increase in surface pressure is not an inherent material property but rather is dependent on the dimensions of the system and also on process parameters such as compression speed. Figure 3 displays constant compression rate surface pressure-area isotherms of Langmuir PLGA films prepared at different initial PLGA surface concentrations. When plotted in the surface pressure vs. area per monomer plane, the film area at the onset of the surface pressure up turn decreases as the initial amount of the polymer spread at the air-water interface is increased; the thicker the film, the smaller area per chain point it requires to be compressed to in order to become glassy, which may appear counter-intuitive. However, the inset of Figure 3 where the same data are presented in plots of surface pressure vs. barrier position offers a more clear picture of the situation; the thicker the film, the smaller amount of deformation (strain) it requires to receive in order to become glassy. It is clear that the surface pressure behavior of the Langmuir PLGA film at high compression is of mechanical origin rather than being caused by an equilibrium-type process.

### **3.3 Dependence of Langmuir Film Glass Transition on Compression Speed**

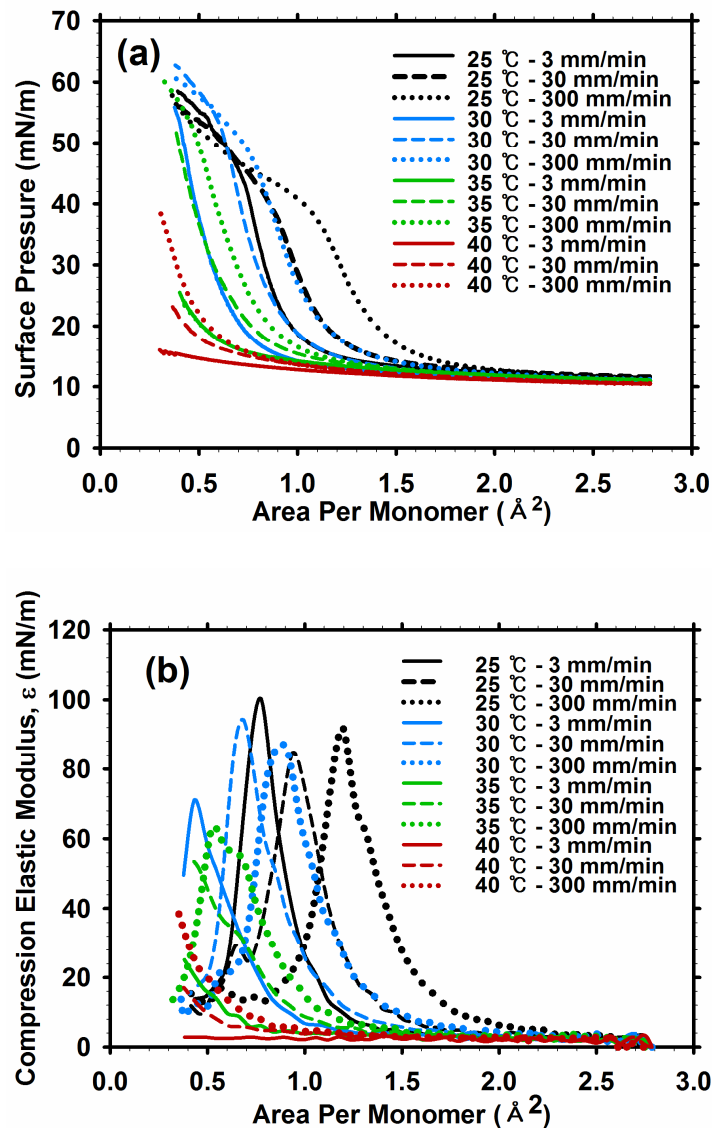


**Figure 4.** (a) Compression rate and temperature dependences of the PLGA monolayer isotherms (PLGA molecular weight: 17.1 kDa). (b) Compression elastic modulus profiles calculated from (a).

In the purely elastic limit, the stress associated with the compression deformation would be completely stored in the film structure in the form of strain energy, which is measured as an increase in surface tension. In a viscoelastic situation, only part of the applied stress will be elastically stored (the rest will be dissipated), and the amount of stored stress will depend on the rate of compression and also time. To demonstrate this aspect, we performed isotherm measurements at varying rates of compression at several different temperatures. The results of

these tests are shown in Figure 4 (a). Interestingly, even at 40 °C, a sharp surface pressure increase was observed if the film was compressed at higher rates ( $> 3$  mm/min), suggesting that the glass transition of the Langmuir PLGA film can be induced by lowering temperature or by increasing the compression rate, and also that therefore the PLGA film is a viscoelastic system.

To our knowledge, there has been no previous report of a compression rate dependent glass transition behavior in Langmuir polymer films. The compression rate dependence of the surface pressure-area isotherm of poly(vinyl acetate) in the high monolayer area regime has been previously discussed.<sup>24</sup> We will propose a possible mechanism for the compression rate dependent glass transition process observed with Langmuir PLGA films in Section 3.5. It is known that hydrostatic (i.e., volumetric) compression/confinement typically causes hardening (and thus increases the glass transition temperatures) of polymeric materials.<sup>25-29</sup> It needs to be clarified that lateral compression of a Langmuir polymer film does not produce volumetrically compressed situations because the material is unbound in the perpendicular direction.

Willard Gibbs has suggested that when the change in the surface area of a liquid affects its surface tension, the liquid surface can behave as an elastic sheet.<sup>30</sup> Langmuir PLGA films appear to represent an example in which the elasticity does not originate from the effect of surface tension. From the data in Figure 4(a), we calculated the compression elastic moduli of the PLGA films ( $\epsilon \equiv -A \frac{d\pi}{dA}$ ); see Figure 4(b) for plots of the modulus data for various temperature and compression rate conditions. As shown in the figure, at 40 °C at the compression rate of 3 mm/min, the compression elastic modulus is negligible, so the PLGA film is in the compressible (i.e., fluid-like) state with no elastic character. Typically, there exists a peak at an intermediate compression point in the compression modulus vs. monolayer area curves; the decay in modulus at high compression is thought to be due to plastic deformation of the films (e.g., the formation

of wrinkled structures). A general trend is that at a given temperature the modulus peak shifts to a higher area per monomer value with increasing compression rate, and when the compression rate is fixed, the peak elasticity occurs at a lower area per monomer with increasing temperature.

### 3.4 Change in Molecular Structural State During Continuous Film Compression

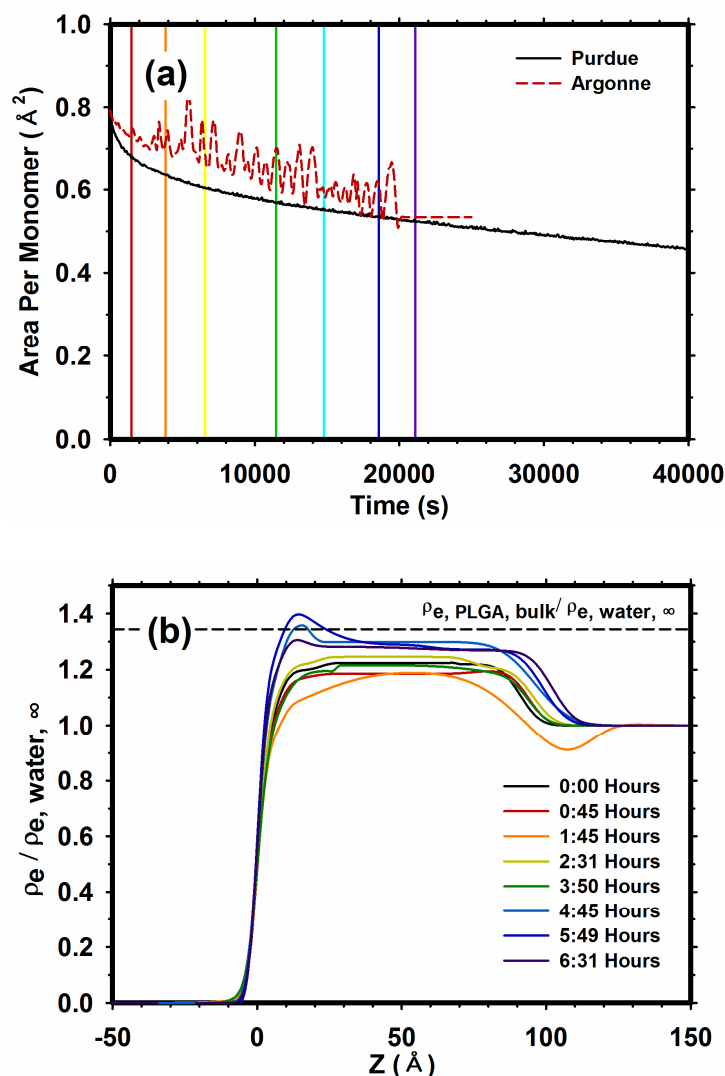


**Figure 5.** (a) Areas of Langmuir PLGA films (pre-compressed to a surface pressure of 30 mN/m) measured as a function of time; during the measurements the surface pressure was kept constant at 30 mN/m (PLGA molecular weight: 17.1 kDa). The black curve was obtained using a Langmuir trough instrument kept in a vibration-free environment. The red curve represents the same measurement performed during XR data collection. The vertical lines denote the time points (i.e., the start times of the XR scans) at which the XR data presented in (b) and also in Figure S5 of the ESI were obtained. (b) The normalized electron density profiles obtained from the XR investigation of the Langmuir PLGA film subjected to the constant surface pressure. The

original XR data from which these electron density curves were constructed are presented in Figure S5 of the ESI. The numbers in the legend indicate the start times of the XR scans (in “hours:minutes”); this time is measured from the time at which the pre-compression process reached the set surface pressure condition (30 mN/m).

In order to probe the molecular structural change that occurs during continuous compression of the Langmuir PLGA film, X-ray reflectivity (XR) measurements were performed on a PLGA film kept at a constant surface pressure of 30 mN/m by adjustment of the film area (at a constant temperature of 25 °C); the monolayer sample was initially prepared at an area of 4 Å<sup>2</sup> per monomer and then compressed (at a rate of 3 mm/min) to the measurement surface pressure of 30 mN/m (which corresponded to a film area of about 0.8 Å<sup>2</sup> per monomer). As shown in Figure 5(a), maintaining the surface pressure at the set level (30 mN/m) required continuous compression of the film, and as a result the film area steadily decreased over time. This procedure was used to imitate (qualitatively) what happens when the Langmuir PLGA film is subjected to a constant rate of compression during a typical isotherm measurement; the XR scan (over the  $q_z$  range from 0.016 to 0.7 Å<sup>-1</sup>) at each area per monomer condition takes about 45 minutes (about 10 minutes for height scans for area search, and then about 35 minutes for an actual reflectivity run), and therefore XR measurements on a Langmuir PLGA film cannot be performed during continuous compression of the film using the same compression rate as used during the isotherm measurements (i.e., 3 mm/min or higher). The black curve in Figure 5(a) is the film area trace measured with time over a 12-hour period; a longer measurement was not possible due to evaporation of the water. This measurement was performed in our Purdue laboratory in a vibration-free environment. Also shown in red in Figure 5(a) is an area relaxation curve obtained during the XR data collection process. XR measurements typically involved adjustment of the vertical and horizontal positions of the trough, and this process caused

perturbation of the surface pressure measurement process, which in turn produced small-scale fluctuations in the area value (red curve); nevertheless the overall decreasing trend in film area was apparent, and it matched the trend in the data obtained in the vibration-free condition (black curve). The normalized XR profiles from these measurements are shown in Figure S5. The overall electron density profiles ( $\rho_e(z)$ ) obtained from the box-model analysis of the XR data (plotted in a normalized form where the  $\rho_e(z)$  quantities are referenced to the electron density of bulk water  $\rho_{e,\text{water},\infty}$ ) are shown in Figure 5(b); the best-fit XR profiles are also presented in Figure S5. As shown in this figure, we observe a trend that the overall electron density of the PLGA film increases with compression. Interestingly, at high compression the PLGA film structure becomes significantly vertically asymmetric; a peak develops on the air-side edge of the electron density profile. Also, it is notable that at high compression the actual maximum electron density value at the peak position becomes comparable to, or even exceeds, the electron density of glassy bulk PLGA, supporting that a dense (i.e., glassy) sublayer is formed on the air side of the Langmuir PLGA film under high lateral compression; the glass transition occurs only within part of the polymer film.

### 3.5 Humidity Dependent Film Glass Transformation

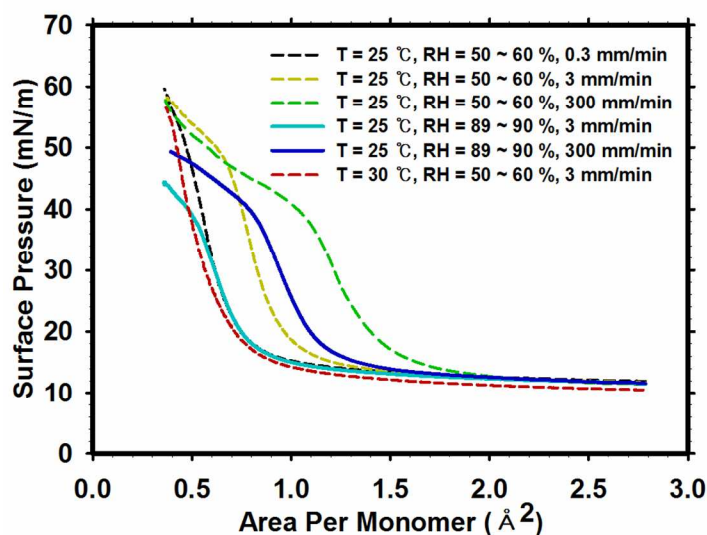


**Figure 6.** Effect of humidity in the air on the constant compression rate isotherm of the Langmuir PLGA film (PLGA molecular weight: 17.1 kDa).

The XR results offer an important clue as to why/how lateral compression induces a transient glassy state in the Langmuir PLGA film. We first need to note that it is known that the presence of water has a plasticizing effect on PLGA with an associated decrease in the glass transition temperature ( $T_g$ ) of bulk PLGA from about 45 °C to about 37 °C.<sup>19</sup> The actual amount of water needed to reduce the  $T_g$  of PLGA to a level of about 37°C is a moisture content in the polymer of about  $1.26 \pm 0.07$  % (w/w); this condition is easily realized when the surrounding air has a relative humidity of 90 % at 25 °C (or a relative humidity of 50 % at 37 °C).<sup>19</sup> We note that the average thickness of this film ( $\approx 11.0$  nm at  $0.8 \text{ \AA}^2$  per monomer) is much smaller than the minimum thickness typically needed for a free-standing polymer film to exhibit a bulk-like glass transition behavior (i.e., on the order of 100 nm),<sup>31, 32</sup> and this information itself might, in fact, look to be able to explain why, for instance, at 40 °C (below the  $T_g$  of bulk PLGA) the air-water Langmuir film of PLGA behaves as a liquid-like material. However, this thickness effect appears

to be unable to explain why then this ultrathin polymer film becomes glassy under rapid compression. At the present, we believe it is mainly the moisture supplied from the subphase (rather than the effect of the thickness) that causes plasticization of the Langmuir PLGA film into a deformable state. Now, when this PLGA film is laterally compressed, what appears to happen (based on the XR results shown in Figure 5(b)) is that this compression produces a newly formed layer of PLGA (on the air side of the polymer film) in which (for some reason – not yet understood) the water content is significantly lower than the rest of the regions and thus the polymer becomes glassy within this dry zone. However, this locally dry condition does not last long, probably because of continuous diffusion of water from the subphase; thus, when the compression is stopped, the Langmuir PLGA film returns to a non-glassy state (as demonstrated by the surface pressure relaxation data taken at 25 °C in Figure S4 of the ESI).

In order to confirm this hypothesized role of humidity in controlling the mechanical property of a Langmuir PLGA film, we performed constant compression rate isotherm measurements at varying environmental humidity conditions. The results of these experiments are presented in Figure 6. It should be noted that in a non-humidity controlled environment the relative humidity within the Plexi glass housing of our Langmuir trough instrument was measured to be typically in the range of 50 to 60 % at 25 °C during the isotherm measurement process; the relative humidity reading typically starts out at about 50 %, and it increases to a level of about 60 % because of the closed environment of the trough chamber. We used a commercial humidifier in order to manually control the relative humidity of the trough chamber to a target level of 90 % at 25 °C. Interestingly, as shown in Figure 6, the PLGA isotherm obtained at 25 °C under 89 – 90 % relative humidity was quite comparable to the curve obtained at a higher temperature of 30 °C and a lower relative humidity of 50 – 60 % (the compression rate was 3 mm/min in both cases).

In a typical non-humidity controlled experiment, we expect that water continuously evaporates from the air side surface of the PLGA film. Under the 50 – 60% relative humidity condition, the  $T_g$  of the PLGA in the air-polymer interfacial region is expected to be  $42.8 \pm 0.6$  °C, whereas in the region closer to the polymer-water interface the  $T_g$  of the water-saturated PLGA will be about 30 °C.<sup>19</sup> This gradient in the  $T_g$  property (and thus the gradient in density) is clearly evidenced by the asymmetric overall electron density profiles shown in Figure 5(b), and is believed to be the cause of the exponential up turn in surface pressure that occurs under continuous compression. Further, the compression rate dependence of the surface mechanical response of the PLGA film appears to imply that the rate of water transfer from the subphase to the PLGA film is normally slower than the rate of water evaporation at the air surface of the PLGA film. Under the fast evaporation condition, fast compression will produce more surface and thus dry regions on the air side of the PLGA film if the water diffusion from the subphase to the PLGA film is slower; in this situation, the dry region near the air surface will transform to a (transient) glassy state, giving rise to an exponential increase in surface pressure (if the temperature is below the  $T_g$  of bulk PLGA). This picture is also supported by the data shown in Figure 6, which shows that a film compression at a rate of 0.3 mm/min under 50 – 60% relative humidity at 25 °C produces an isotherm that is similar to the one obtained at both higher compression rate of 3 mm/min and relative humidity of 89 – 90% at 25 °C.

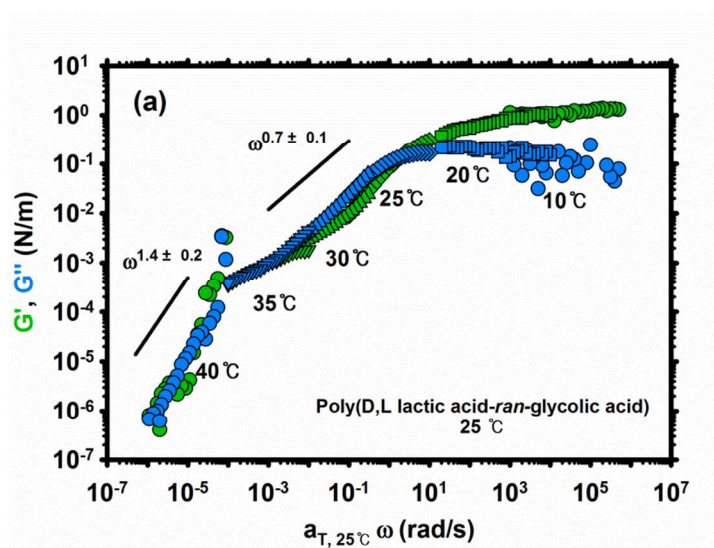
To our knowledge, previously there has been no study that investigated the effect of environmental humidity on the properties of Langmuir polymer films. Langmuir films of poly(vinyl acetate) (PVA) have previously been studied;<sup>24</sup> for PVA, the air-water interface provides a “good solvent” environment in which the polymer exhibits a two dimensional Flory exponent of 0.79.<sup>6</sup> The results of this previous study demonstrated that the glass transition

behavior of a Langmuir PVA film clearly deviates from what is observed with bulk PVA. This difference was thought to be due to the confinement of the chains to small air-water interfacial regions in the monolayer situation.<sup>24, 33</sup> Interestingly, a recent study suggests that even single polymer chains can exhibit glassy dynamics commensurate with those observed in the bulk environment.<sup>2</sup> Water has been reported to have a plasticizing effect on PVA.<sup>34</sup> Taken together, we suspect that the main cause of the plasticization of PVA in Langmuir monolayer form is the saturation of the material with water from the subphase. Therefore, it is also expected that Langmuir PVA films would exhibit a compression rate-dependent glass transition behavior in the low area per monomer regime (similarly to Langmuir PLGA films); currently, study is underway to confirm this effect.

### 3.7 Interfacial Rheological Properties of the Langmuir PLGA Film

Interfacial rheological characterizations were performed at six different temperatures (10, 20, 25, 30, 35 and 40 °C) on the air-water interfacial films of PLGA prepared by spreading the polymer on the water surface directly to an area per monomer of  $0.8 \text{ \AA}^2$  initially at 25 °C (Figure 7(a)). It should first be noted that (as discussed in Section 3.2) this as-spread sample prepared directly at  $0.8 \text{ \AA}^2$  per monomer at 25 °C shows a surface pressure ( $\approx 11.6 \text{ mN/m}$ ) that is significantly lower than the surface pressure values obtained with compressed samples (Figure 3). Also, as shown in Figure S6, the as-spread sample shows an electron density profile that is significantly different from the sample initially prepared at  $4 \text{ \AA}^2$  per monomer and then compressed (at a rate of 3 mm/min) to the final area of  $0.8 \text{ \AA}^2$  per monomer. This difference is thought to be due to the formation of large (macroscopic) unspread domains of PLGA within the Langmuir film in the as-spread situation (these large domains occupy a negligible fraction of the total area of the film and thus make negligible contributions to the overall XR signal<sup>4</sup>); these

macroscopic features were often visible even with bare eye at film areas less than  $0.8 \text{ \AA}^2$  per monomer. The exact role that this heterogeneity plays in the overall mechanical behavior of Langmuir PLGA films remains to be further characterized. It needs to be pointed out that despite the existence of heterogeneity the macroscopic properties of Langmuir PLGA films (such as the surface mechanical and rheological properties) were highly reproducible from measurement to measurement. Currently, a combined macro and micro rheological study is in progress to characterize detailed structural and dynamic properties of heterogeneous domains and their influences on the mechanical properties of Langmuir PLGA films; both compressed and as-spread samples are being investigated.



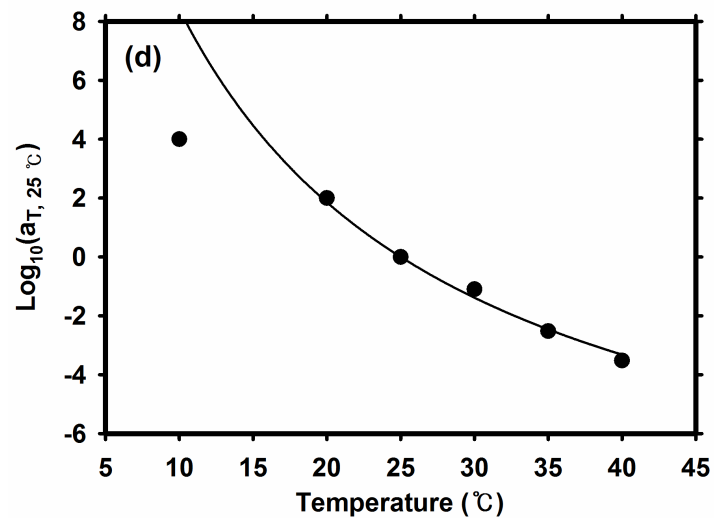
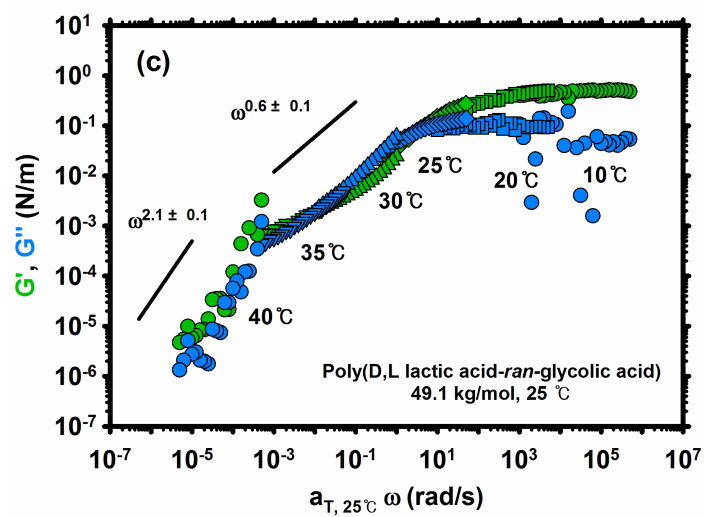
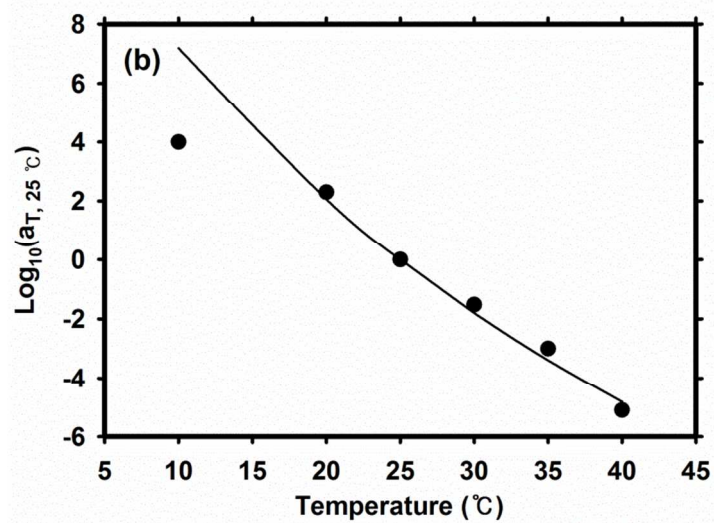


**Figure 7.** (a) Time-temperature superposition of linear dynamic elastic and viscous moduli ( $G'$  and  $G''$ , respectively) for as-spread PLGA films at  $0.8 \text{ \AA}^2$  area per monomer at  $25 \text{ }^\circ\text{C}$  (PLGA molecular weight: 17.1 kDa). At  $40 \text{ }^\circ\text{C}$  the raw phase angles were either close to or above  $175$  degrees; so the measurement was not completely reliable. At all lower temperatures ( $35, 30, 25, 20$  and  $10 \text{ }^\circ\text{C}$ ), the Boussinesq numbers were estimated to be greater than  $10^3$ ; therefore, it was unnecessary to make corrections for subphase flow effects, because such corrections will have negligible effects on the data.<sup>35</sup> (b) Temperature dependence of the horizontal shift factors used to obtain the  $G'$  and  $G''$  master curves shown in (a) and the corresponding fit to the Williams-Landel-Ferry (WLF) equation. The best fit WLF parameter values were  $C_1 = 29.2$  and  $C_2 = 75.9 \text{ }^\circ\text{C}$ . (c) The same measurements as in (a) were repeated with a higher molecular weight PLGA (49.1 kDa). (d) The temperature-dependent frequency shift factors used in (c). The best fit WLF parameter values were  $C_1 = 11.0$  and  $C_2 = 34.6 \text{ }^\circ\text{C}$ .

Oscillatory shear stress sweep measurements were first performed to determine the linear viscoelastic torque limit for an as-spread PLGA film at  $0.8 \text{ \AA}^2$  per monomer at each temperature condition. Based on the results from these tests (data at  $25 \text{ }^\circ\text{C}$  demonstrated in Figure S7), linear frequency sweep measurements were performed over an angular frequency range of  $0.1 - 10$  rad/s under a controlled-stress mode of testing at a constant torque of  $0.5 \text{ } \mu\text{N}\cdot\text{m}$ . Both descending and ascending frequency sweeps were performed at all temperatures examined ( $10, 20, 25, 30, 35$  and  $40 \text{ }^\circ\text{C}$ ). Linear oscillatory frequency sweep results were confirmed to be independent of the direction of the frequency sweep; data were obtained by two successive frequency sweep runs on a single sample loading: a descending sweep from  $10$  to  $0.1$  rad/s followed by an ascending sweep from  $0.1$  to  $10$  rad/s. We found that under this frequency range setting, even if the measurement sequence was reversed (i.e., first an ascending sweep, and then a descending sweep over the same range of frequency) the modulus values (i.e.,  $G'$  and  $G''$ ) were identical between the two types of sweeps (data not shown). However, when the measurement frequency range was increased to  $0.01 - 100$  rad/s (data not shown), the moduli of the descending branches (both  $G'$  and  $G''$ ) were found to be, respectively, significantly higher than those of the ascending

branches, and such effect was observed to be increasingly pronounced with increasing oscillation frequency.

Most importantly, as shown in the time-temperature superposed form in Figure 7(a), the as-spread PLGA film at  $0.8 \text{ \AA}^2$  per monomer at  $25 \text{ }^\circ\text{C}$  shows a non-Newtonian (viscoelastic) response. One might argue that in Langmuir polymer films, viscoelasticity can occur due to two possible conditions: the entanglement of the chains, and the existence of glassy domains within the Langmuir PLGA film. In fact, the viscoelasticity (under dilation/compression or shear) due to the entanglement might itself produce qualitatively similar effects in the surface pressure-area isotherm data (i.e., an exponential increase in surface pressure under rapid compression) and also in the frequency sweep interfacial rheology data (a viscoelastic crossover); at thicknesses about 10 nm, entanglement might play a role in determining the mechanical properties of the Langmuir PLGA film because the bulk gyration radius of the 17.1-kDa PLGA is estimated to only about 3.4 nm.<sup>36</sup> However, the viscoelasticity due to entanglement by itself cannot explain, for instance, the observed effect of humidity on the mechanical behavior of the PLGA film. Further, the relaxation behavior of the Langmuir PLGA film in the transition zone (i.e.,  $G'$ ,  $G'' \sim \omega^{0.7}$ ) clearly deviates from what is expected for the terminal relaxation of an entangled polymer melt ( $G' \sim \omega^2$ , and  $G'' \sim \omega^1$ ). Polydispersity cannot explain this behavior either.<sup>37</sup> Instead, the observed scaling ( $G'$ ,  $G'' \sim \omega^{0.7}$ ) appears to correspond more closely to the well-known behavior of polymers and colloids slightly above their glass transition temperatures.<sup>38, 39</sup> Also of note an angular deformation frequency of, for instance, 0.01 rad/s approximately corresponds to a linear deformation velocity of 3 mm/min. Therefore, this surface rheology result is consistent with the glassy response observed in surface pressure measurements; we expect that a glassy polymer film would show a viscoelastic rheological response, in analogy to bulk glassy materials.<sup>38</sup>

In an effort to further elucidate the origin of the elasticity of the Langmuir PLGA film, we repeated the linear oscillatory frequency sweep measurements with a higher molecular weight PLGA (having a number-average molecular weight of 49.1 kg/mol) (data shown in Figure 7(c)); if the elastic modulus plateau indeed occurs due to the glassy nature of the PLGA film, the onset frequency for relaxation ( $\omega_0$ ) (at which  $G'$  starts becoming comparable to or less than  $G''$  as  $\omega$  is decreased) should be independent of polymer molecular weight; if the  $G'$  plateau arises due to chain entanglements or other single chain effects, the onset frequency would exhibit a dependence on molecular weight. As can be seen from comparison between Figures 7(a) and 7(c), the time-temperature superposed linear viscoelastic moduli data for the 17.1 and 49.1-kDa PLGA materials were found to be indistinguishable with respect to polymer molecular weight. These results indicate that the observed viscoelastic behavior does not reflect any effects of global single-chain relaxation processes, but it reflects the local segment dynamics of the chain; these results support the notion that the observed elasticity is due to the glassy nature of the Langmuir PLGA film.

From the data shown in Figure 7, it is also possible to calculate the elastic energy density stored in the PLGA film under oscillatory shear; from the plateau modulus ( $G_p \approx 1$  N/m, Figure 7(A)) and the film thickness at  $0.8 \text{ \AA}^2$  area per monomer ( $L \approx 10$  nm, Figure 1(B)), we estimate the shear energy density of the Langmuir PLGA film to be  $E \approx G_p/L \approx 10^8 \text{ J/m}^3$ . This value is quite comparable to the reported shear modulus of bulk glassy PLGA ( $G \approx 2 \times 10^8 \text{ J/m}^3$  at  $20^\circ\text{C}$ <sup>40</sup>). Therefore, it appears that in the direction of shear, the 10-nm thick PLGA film is almost as hard as bulk glassy PLGA. The entanglement modulus of bulk PLGA is only in the order of  $10^6 \text{ J/m}^3$  (estimated on the basis of the literature data for poly(lactic acid)<sup>41</sup> and poly(glycolic acid)<sup>42</sup>).

Therefore, chain entanglement is unable to explain the observed elasticity of the Langmuir PLGA film.

#### 4. Conclusions

Extensive experimental investigations (including surface pressure-area isotherm, X-ray reflectivity and interfacial rheological measurements) were performed in order to elucidate the molecular mechanisms responsible for the transient glass transition behavior observed with highly compressed Langmuir PLGA films. The combined results suggest the following explanation. In the low area per monomer regime the Langmuir PLGA film exists in a highly collapsed (multi layered) structure. Lateral compression normally increases the average thickness of the PLGA film, because PLGA is insoluble in water. However, PLGA typically absorbs a finite amount of water, and water has a plasticizing effect on PLGA; the moisture lowers the  $T_g$  of the PLGA. When the PLGA film is compressed at a sufficiently fast speed, this process produces dry regions on the air side of the polymer film at a rate higher than the re-moisturization rate of the polymer film. This situation creates a gradient of glass transition character across the vertical dimension of the Langmuir PLGA film. At temperatures below the  $T_g$  of bulk PLGA, the top dry regions of the PLGA film therefore undergo glass transition to become solid, giving rise to a sharp upturn in the surface pressure under compression. If the compression is stopped, the whole PLGA film becomes plasticized again due to the continuous diffusion of water from the subphase solution; accordingly, the surface pressure relaxes over time back to a level corresponding to the as-spread Langmuir film situation for a given area per monomer condition (as-spread PLGA films are non-glassy even when prepared at low area per monomer conditions). This explanation is also able to rationalize the observation that the glass

transition of a Langmuir PLGA film is suppressed in high humidity environments and also when the compression is sufficiently slow. The interfacial rheology study results suggest that as-spread PLGA films are also in a glassy state when subjected to deformation.

We believe that this humidity-dependent compression-induced glass transition behavior of air-water interfacial polymer films is not specific to the particular polymer studied here (PLGA). We speculate that any water-insoluble polymer having a bulk  $T_g$  slightly higher than room temperature will likely show a similar behavior at the water surface. To our knowledge, the environmental humidity has not previously been recognized as an important factor that determines the properties of the air-water interfacial monolayers of polymers (and lipids). Further study is required to fully understand this phenomenon. PLGA has been commonly used as a carrier material for pulmonary delivery of drugs.<sup>43,44</sup> We believe the findings of this present study has useful implications for understanding the behavior of PLGA in the lung environment where humidity is known to be high (close to 100 % in relative humidity<sup>45</sup>).

#### ASSOCIATED CONTENT

**Electronic Supplementary Information (ESI) Available:** The procedure for the XR data analysis (Section S1); surface pressure vs. area isotherms at two different Wilhelmy plate orientations (Figure S1); XR profiles from PLGA monolayers at different area conditions (Figure S2); best fit parameters for the XR profiles shown in Figure S2 (Table S1); thicknesses of the PLGA monolayer at various area per chain conditions (Figure S3); surface pressure and surface area relaxation profiles of compressed PLGA films (Figure S4); a time series of XR profiles from a Langmuir PLGA film at a constant surface pressure (Figure S5); best fit parameters for the XR profiles shown in Figure S5 (Table S2); electron density profiles of compressed vs. as-

spread PLGA films (Figure S6); determination of the linear viscoelastic torque limit for Langmuir PLGA films (Figure S7).

## AUTHOR INFORMATION

### Corresponding Author

\*E-mail: yywon@ecn@purdue.edu

### Notes

The authors declare no competing financial interest

## ACKNOWLEDGMENT

We would like to thank the U.S. National Science Foundation (NSF) for providing financial support for this research (DMR-0906567, and CBET-1264336). ChemMatCARS Sector 15 at the Advanced Photon Source of Argonne National Laboratory (where the XR measurements reported in this paper were performed) is supported by the NSF under grant number NSF/CHE-1346572. The use of the Advanced Photon Source, an Office of Science User Facility operated for the U.S. Department of Energy (DOE) Office of Science by Argonne National Laboratory, is supported by the U.S. DOE under Contract No. DE-AC02-06CH11357.

## REFERENCES

1. F. Monroy, L. R. Arriaga and D. Langevin, *Physical Chemistry Chemical Physics*, 2012, **14**, 14450-14459.
2. M. Tress, E. U. Mapesa, W. Kossack, W. K. Kipnusu, M. Reiche and F. Kremer, *Science*, 2013, **341**, 1371-1374.

3. A. R. Esker, C. Kim and H. Yu, in *Functional Materials and Biomaterials*, Springer Berlin Heidelberg, 2007, vol. 209, ch. 113, pp. 59-110.
4. K. N. Witte, S. Kewalramani, I. Kuzmenko, W. Sun, M. Fukuto and Y.-Y. Won, *Macromolecules*, 2010, **43**, 2990-3003.
5. D. Poupinet, R. Vilanove and F. Rondelez, *Macromolecules*, 1989, **22**, 2491-2496.
6. R. Vilanove and F. Rondelez, *Physical Review Letters*, 1980, **45**, 1502-1505.
7. R. Vilanove, D. Poupinet and F. Rondelez, *Macromolecules*, 1988, **21**, 2880-2887.
8. M. Rubinstein and R. H. Colby, eds., *Polymer Physics*, Oxford University Press, New York, 2003.
9. M. J. Stephen and J. L. McCauley, *Phys. Lett. A*, 1973, **A 44**, 89-90.
10. P. J. Flory, *Cornell University Press*, 1953.
11. M. Kawaguchi, S. Komatsu, M. Matsuzumi and A. Takahashi, *Journal of Colloid and Interface Science*, 1984, **102**, 356-360.
12. M. Kawaguchi, A. Yoshida and A. Takahashi, *Macromolecules*, 1983, **16**, 956-961.
13. A. Takahashi, A. Yoshida and M. Kawaguchi, *Macromolecules*, 1982, **15**, 1196-1198.
14. H.-W. Park, J. Choi, K. Ohn, H. Lee, J. W. Kim and Y.-Y. Won, *Langmuir*, 2012, **28**, 11555-11566.
15. D. J. Crisp, *Journal of Colloid Science*, 1946, **1**, 49-70.
16. D. J. Crisp, *Journal of Colloid Science*, 1946, **1**, 161-184.
17. N. B. Vargaftik, B. N. Volkov and L. D. Voljak, *Journal of Physical and Chemical Reference Data*, 1983, **12**, 817-820.
18. H. Lee, V. Tsouris, Y. Lim, R. Mustafa, J. Choi, Y. H. Choi, H. W. Park, M. Meron, B. H. Lin and Y. Y. Won, *Soft Matter*, 2014, **10**, 3771-3782.
19. P. Blasi, S. S. D'Souza, F. Selmin and P. P. DeLuca, *Journal of Controlled Release*, 2005, **108**, 1-9.
20. K. S. Anderson and M. A. Hillmyer, *Macromolecules*, 2004, **37**, 1857-1862.
21. S. Y. Gao, Y. P. Koh and S. L. Simon, *Macromolecules*, 2013, **46**, 562-570.
22. J. Hur, K. N. Witte, W. Sun and Y.-Y. Won, *Langmuir*, 2009, **26**, 2021-2034.
23. K. N. Witte, J. Hur, W. Sun, S. Kim and Y.-Y. Won, *Macromolecules*, 2008, **41**, 8960-8963.
24. E. Spigone, G.-Y. Cho, G. G. Fuller and P. Cicuta, *Langmuir*, 2009, **25**, 7457-7464.
25. M. Alcoutlabi and G. B. McKenna, *Journal of Physics: Condensed Matter*, 2005, **17**, R461.
26. E. Gacoin, C. Fretigny, A. Chateauminois, A. Perriot and E. Barthel, *Tribology Letters*, 2006, **21**, 245-252.
27. E. Jones Parry and D. Tabor, *Journal of Materials Science*, 1973, **8**, 1510-1516.
28. D. Machon, F. Meersman, M. C. Wilding, M. Wilson and P. F. McMillan, *Progress in Materials Science*, 2014, **61**, 216-282.
29. W. Xu, N. Chahine and T. Sulchek, *Langmuir*, 2011, **27**, 8470-8477.
30. J. W. Gibbs, *The Collected Works of J. Willard Gibbs*, 1948.
31. J. A. Forrest and J. Mattsson, *Physical Review E*, 2000, **61**, R53-R56.
32. A. Bansal, H. Yang, C. Li, K. Cho, B. C. Benicewicz, S. K. Kumar and L. S. Schadler, *Nat Mater*, 2005, **4**, 693-698.
33. F. Monroy, F. Ortega and R. G. Rubio, *The European Physical Journal B - Condensed Matter and Complex Systems*, 2000, **13**, 745-754.
34. C. Wu, *Polymer*, 2010, **51**, 4452-4460.

35. S. Vandebriel, A. Franck, G. G. Fuller, P. Moldenaers and J. Vermant, *Rheologica Acta*, 2010, **49**, 131-144.
36. A. E. Tonelli and P. J. Flory, *Macromolecules*, 1969, **2**, 225-&.
37. S. H. Wasserman and W. W. Graessley, *Journal of Rheology*, 1992, **36**, 543-572.
38. J. D. Ferry, *Viscoelastic Properties of Polymers*, John Wiley & Sons, 1980.
39. P. Sollich, *Physical Review E*, 1998, **58**, 738-759.
40. S. H. Choi and T. G. Park, *Journal of Biomaterials Science-Polymer Edition*, 2002, **13**, 1163-1173.
41. J. R. Dorgan, J. S. Williams and D. N. Lewis, *Journal of Rheology*, 1999, **43**, 1141-1155.
42. E. Gautier, P. Fuertes, P. Cassagnau, J. P. Pascault and E. Fleury, *Journal of Polymer Science Part a-Polymer Chemistry*, 2009, **47**, 1440-1449.
43. J. C. Sung, B. L. Pulliam and D. A. Edwards, *Trends in Biotechnology*, 2007, **25**, 563-570.
44. N. Tsapis, D. Bennett, B. Jackson, D. A. Weitz and D. A. Edwards, *Proceedings of the National Academy of Sciences*, 2002, **99**, 12001-12005.
45. G. A. Ferron, B. Haider and W. G. Kreyling, *Bulletin of Mathematical Biology*, 1985, **47**, 565-589.